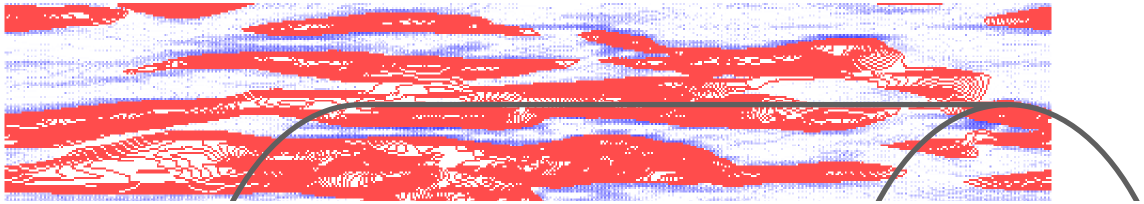

Colloquium in honour of Geneviève Comte-Bellot

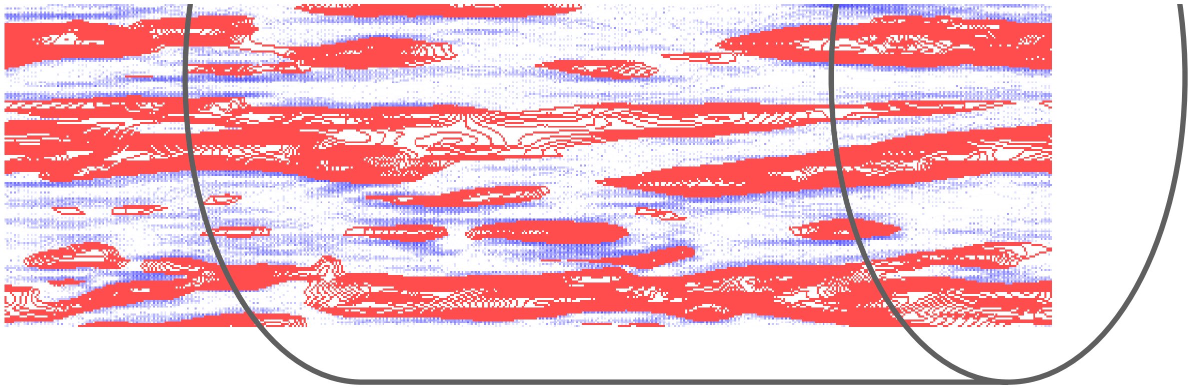

Compressible Turbulent Channel & Pipe Flow: Similarities and Differences

Rainer Friedrich, TU München

Compressible turbulent flows

- Motivation

  Compressible turbulent flows are an important element of high-speed flight

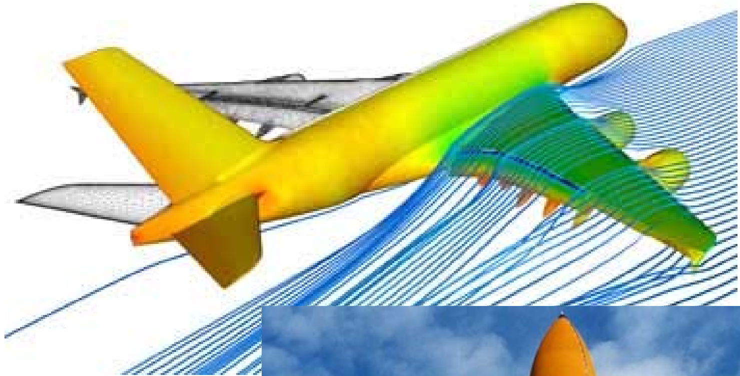

Study of compressible turbulent flows

Names from the early days:

Yaglom (1948): eqs. for 2-point correlations
van Driest (1951): transformation
Kovasznay (1953): exp., modes of compressible turbulence
Morkovin (1961): hypothesis, SRA

Still many open questions:

Measurement difficult...
DNS: important contributions since the 80s

Literature:

Review articles: Bradshaw (1977), Lele (1994)
Agardographs: Fernholz & Finley (1977)
Books: Smits & Dussauge (2006), Chassaing et al. (2002), Gatski & Bonnet (2009), Garnier, Sagaut, Adams (2009)

DNS of compressible channel and pipe flow

- Why spending time with so simple flows?

  Understanding the physical mechanisms that explain similarities & differences between plane & axisymmetric flows forms a first step towards improved turbulence modelling

  Isolating such mechanisms needs simplifications such as e.g. fully-developed flow

Contents

DNS of supersonic channel and pipe flow

- Some computational details
- Compressibility effects
- Comparison of mean flow/Reynolds stresses
- Comparison of Reynolds stress budgets
- Analysis of pressure fields

Some computational details

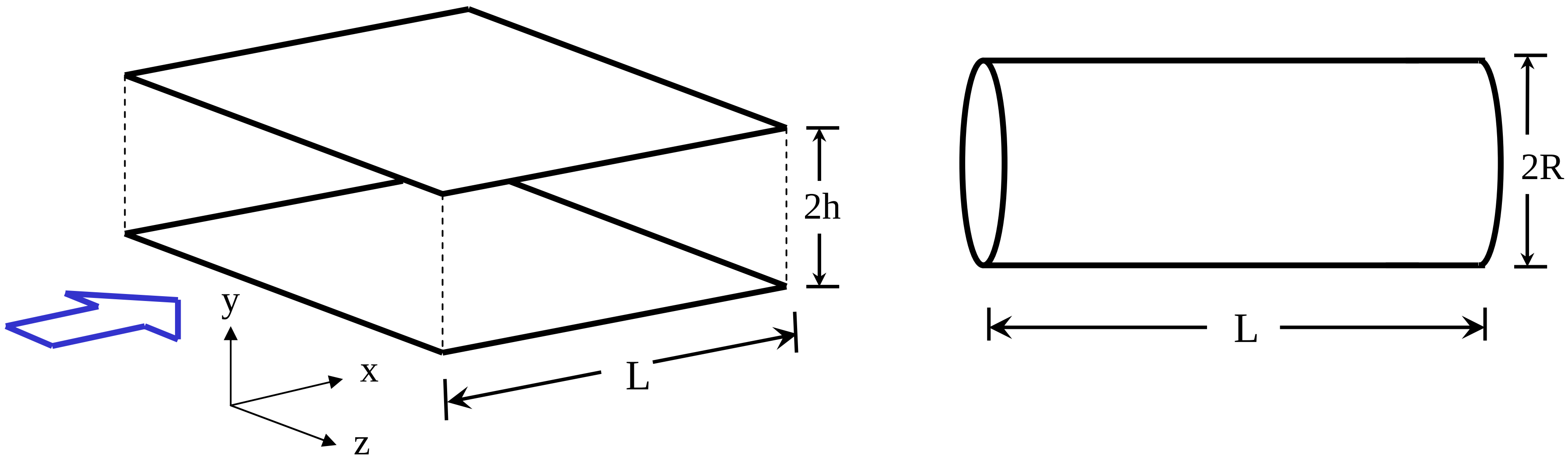

Cartesian/cylindrical coordinates
Treatment of axis singularity as in Mohseni & Colonius (JCP, 2000)
Compact 5th order LD upwind schemes (Adams-Shariff, JCP, 1996)
Compact 6th order central schemes (Lele, JCP, 1992)
3rd order low-storage RK scheme

Some computational details

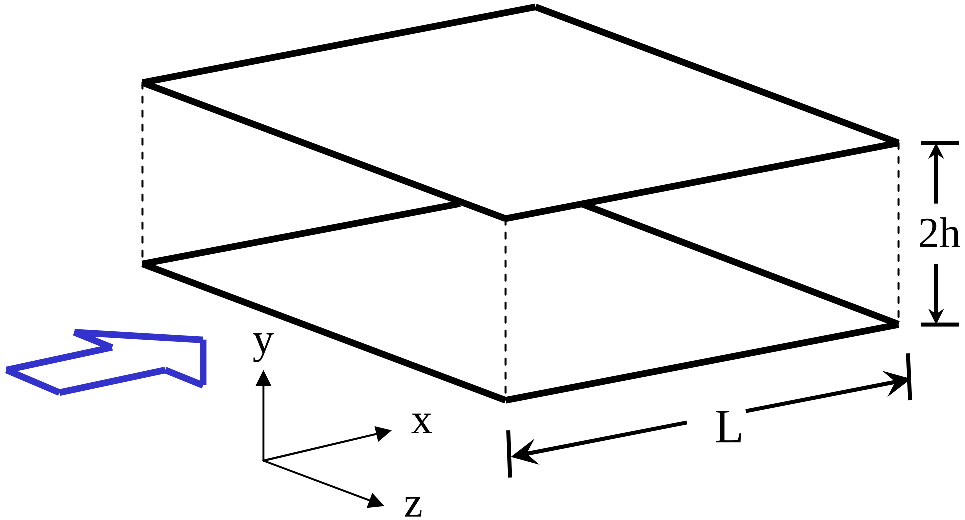

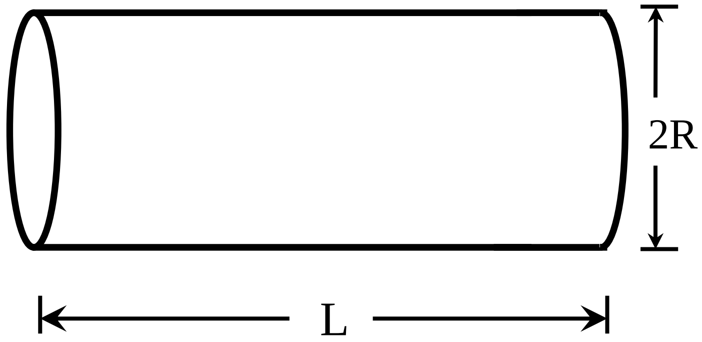

Flow	Re_τ	M_τ	Re_m	M_m	L×H×B	Grid
channel	246	0.078	2986	1.26	4πh×2h×4πh/3	192×151×128
pipe	245	0.077	3181	1.30	10R×R×2Rπ	256×91×128

$$Re_\tau = \rho_w u_\tau l / \mu_w, \quad M_\tau = u_\tau / \sqrt{\gamma R T_w}, \quad Re_m = \rho_m u_m l / \mu_w, \quad l = h, R, \quad \rho_m u_m = \int_0^1 \overline{\rho u}\, d(y/h)$$

Previous work

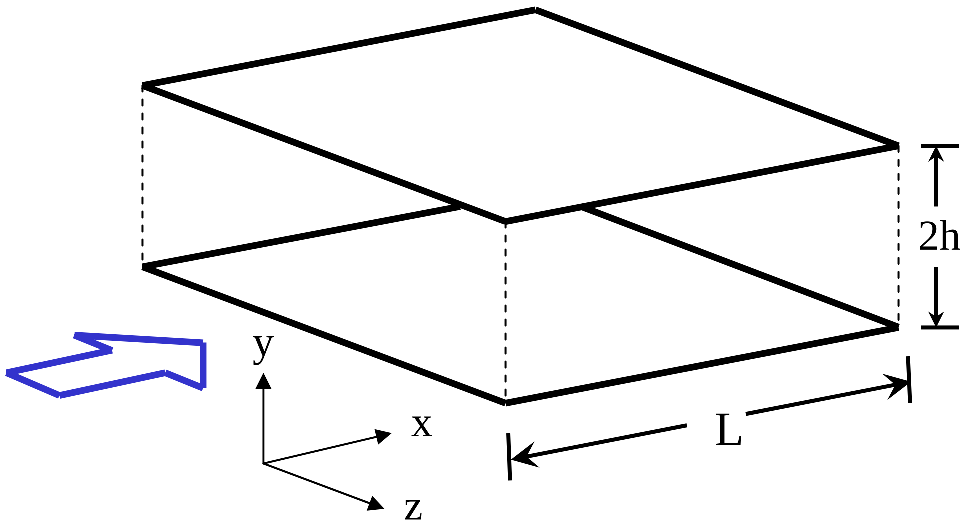

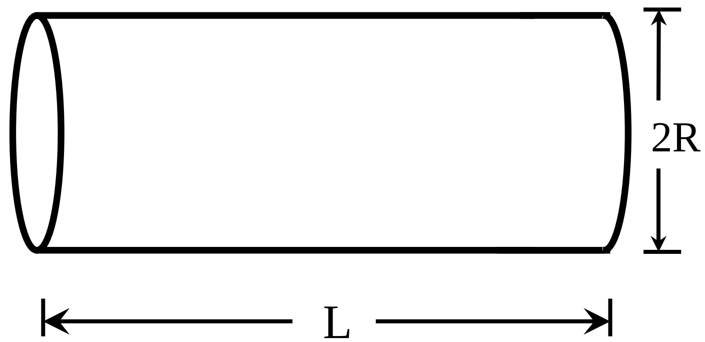

Coleman et al. (JFM 305, 1995)
Huang et al. (JFM 305, 1995)
Morinishi et al. (JFM 502, 2004)
Foysi et al. (JFM 509, 2004)

Ghosh et al. (IJHFF 29, 2008)

Previous work

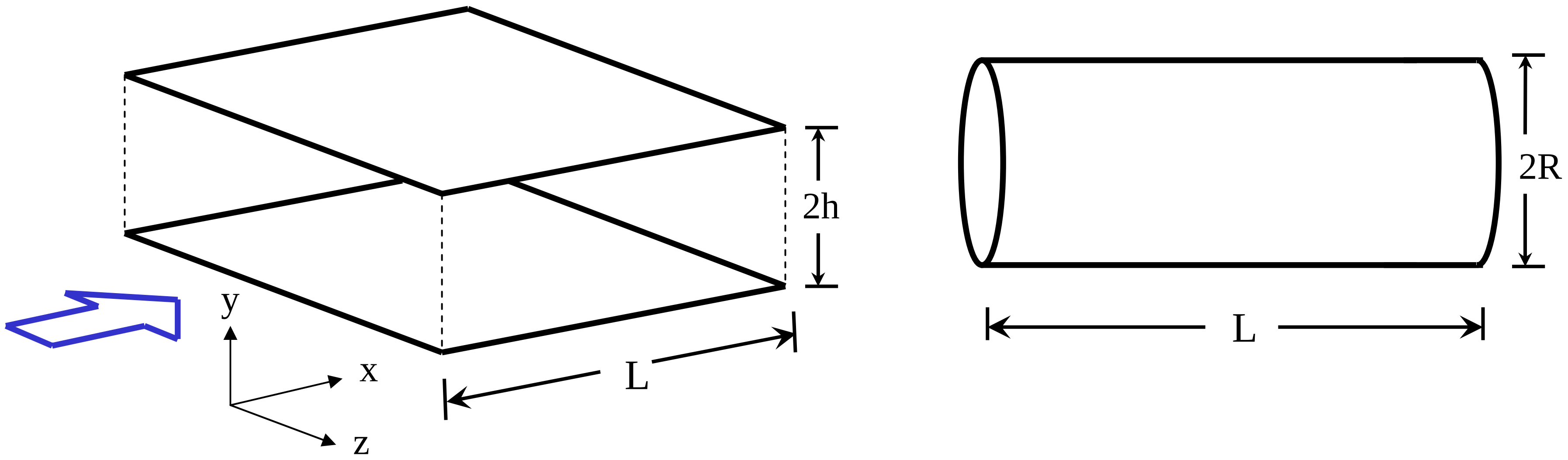

Similarities and differences between incompressible channel & pipe flow:

Schlichting (1968): Similarity between velocities not perfect

Wosnik et al. (JFM 2000): Theory for vel. & skin friction, Re effects

Nieuwstadt & Bradshaw (1997): Similarity fails beyond 2nd order moments

Compressibility effects

Supersonic flow: isothermal walls

Sharp wall-normal gradients of mean density and temperature: mean property variations

Van Driest transformation is successful. SRA needs modification

Mean dilatation effects negligible

Pressure-dilatation and compressible dissipation rate (intrinsic compressibility effects) are unimportant

Density variations responsible for change in pressure-strain correlation and Reynolds stress anisotropy

Comparison of mean flow variables

- Viscous and Reynolds shear stresses

(normalized with inner variables)

$$\frac{\overline{\mu}}{\mu_w}\frac{d\overline{u}^+}{dy^+} - \frac{\overline{\rho u'' v''}}{\overline{\tau}_w} = 1 - \frac{y^+}{l^+} = 1 + a y^+ \overline{p}_x^+$$

$$l^+ = \begin{cases} h^+, & a = 1, \quad \overline{p}_x^+ = -1/h^+, \\ R^+, & a = 1/2, \quad \overline{p}_x^+ = -2/R^+, \end{cases}$$

$$\overline{p}_x^+ = \frac{\mu_w}{\overline{\rho}_w u_\tau \overline{\tau}_w}\frac{d\overline{p}}{dx}, \quad \overline{\tau}_w = \overline{\rho}_w u_\tau^2.$$

R^+ : Kármán number

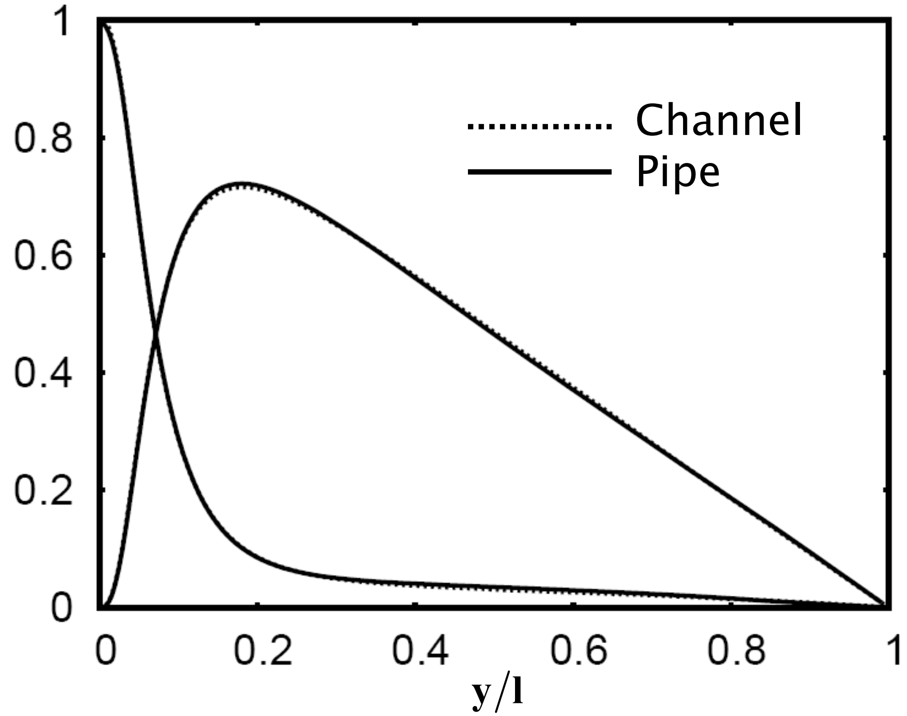

Comparison of mean flow variables

- Mean streamwise velocity

Taylor series expansion for viscous sublayer:

$$\overline{u}^+ = \underbrace{\int_0^{y^+}\frac{\mu_w}{\overline{\mu}}dy^+}_{A} \underbrace{- \int_0^{y^+}\frac{\mu_w}{\overline{\mu}}\frac{y^+}{l^+}dy^+}_{B} + \frac{\sigma}{6}\int_0^{y^+}\frac{\mu_w}{\overline{\mu}}y^{+3}dy^+ + \ldots, \qquad \sigma = \frac{3}{\overline{\tau}_w}\left[\left.\overline{\frac{\partial\rho u''}{\partial y^+}\frac{\partial^2 v''}{\partial y^{+2}}}\right|_w + \left.\overline{\frac{\partial^2\rho u''}{\partial y^{+2}}\frac{\partial v''}{\partial y^+}}\right|_w\right].$$

Pressure-gradient term looses importance at high Re_τ

$$\overline{u}^+ = y^+ - \frac{y^{+2}}{2l^+} + \ldots$$

Incompressible isothermal flow

Differences in the core region

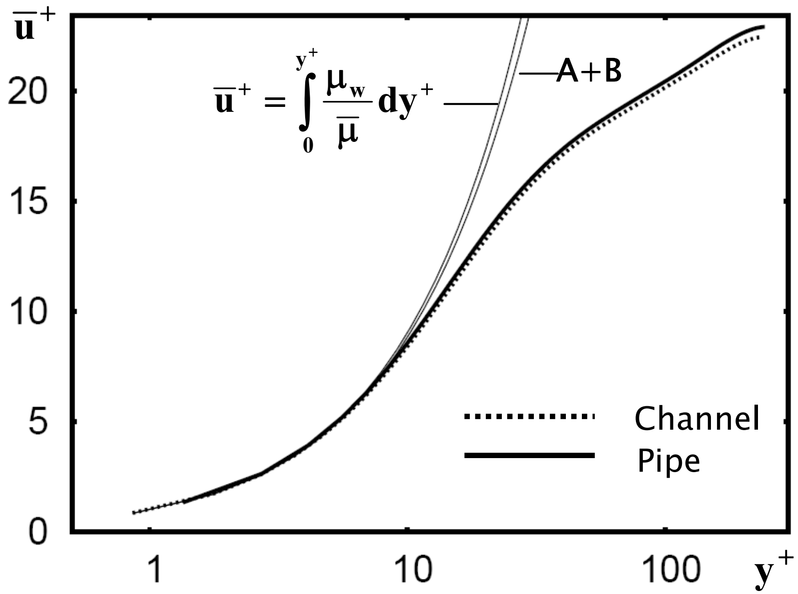

Comparison of mean flow variables

- Mean pressure

Integrated wall-normal momentum balance:

$$\overline{p} = \overline{p}_w - \overline{\rho v''v''} - \int_0^y \left(\overline{\rho v''v''} - \overline{\rho w''w''}\right)\frac{dy}{(R-y)} \quad \textbf{(pipe)}, \qquad \overline{p} = \overline{p}_w - \overline{\rho v''v''} \quad \textbf{(channel)}$$

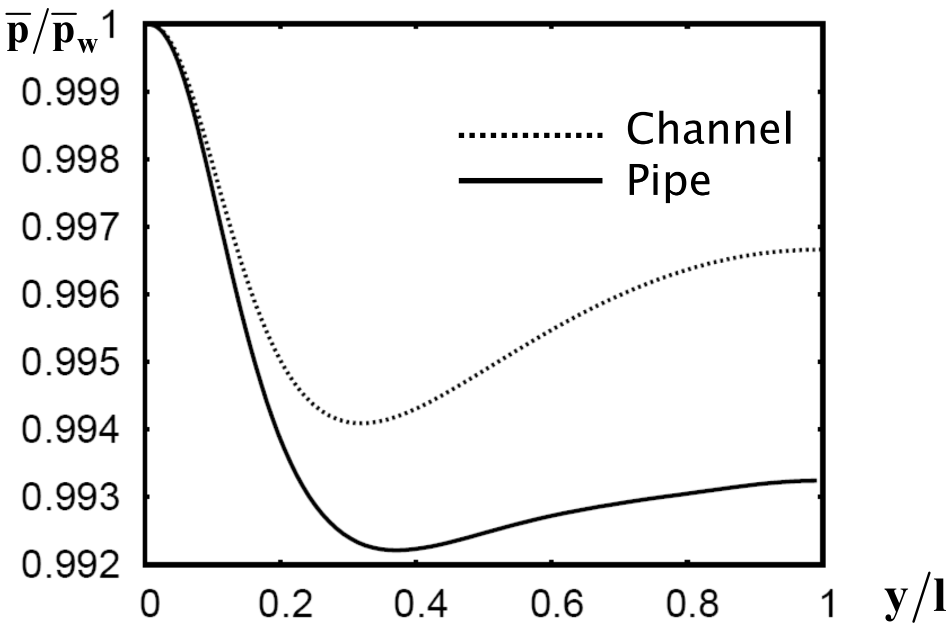

Differences due to transverse curvature.
Wall-normal pressure gradients are small compared to density & temperature gradients

Comparison of mean flow variables

- Mean density and temperature

  Integrated mean energy balance (pipe):

$$\left(1-\frac{y^+}{R^+}\right)\underbrace{\left(\frac{\gamma}{Pr}\frac{\overline{\lambda}}{\lambda_w}\frac{d\left(\overline{T}/T_w\right)}{dy^+}-\frac{\overline{\rho v''T''}}{\rho_w u_\tau T_w}\right)}_{\text{mol. heat flux} \qquad \text{turb. heat flux}}+\underbrace{\gamma B_q}_{\text{wall heat fl.}} \cong -\gamma(\gamma-1)M_t^2\int_0^{y^+}\left(1-\frac{y^+}{R^+}\right)\underbrace{\left(\frac{\overline{\mu}}{\mu_w}\left(\frac{d\overline{u}^+}{dy^+}\right)^2+\varepsilon^+\right)}_{\text{direct \& turb. dissipation}}dy^+ + \text{h.o.t.}$$

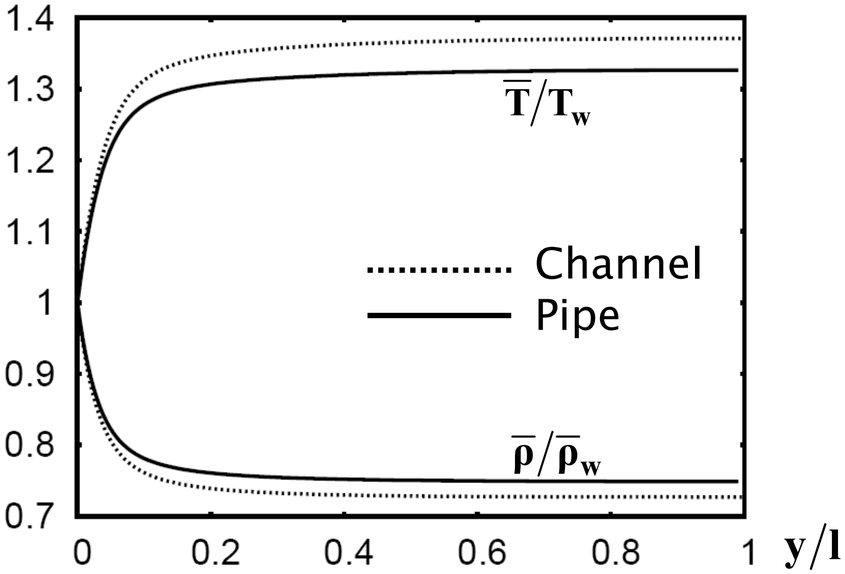

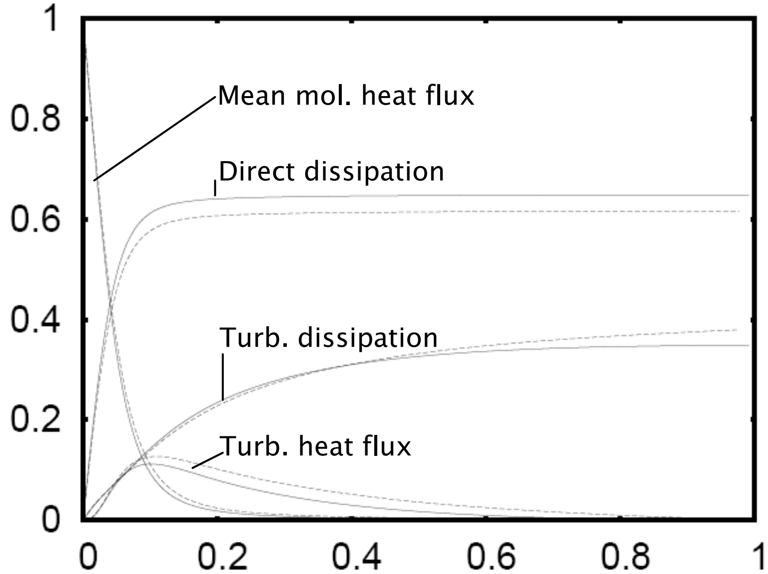

Differences due to transverse curvature...

Comparison of Reynolds stresses

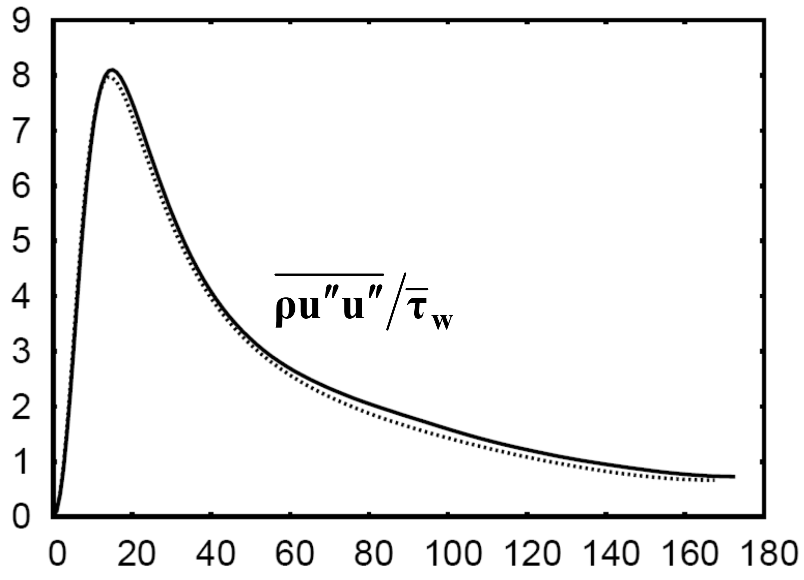

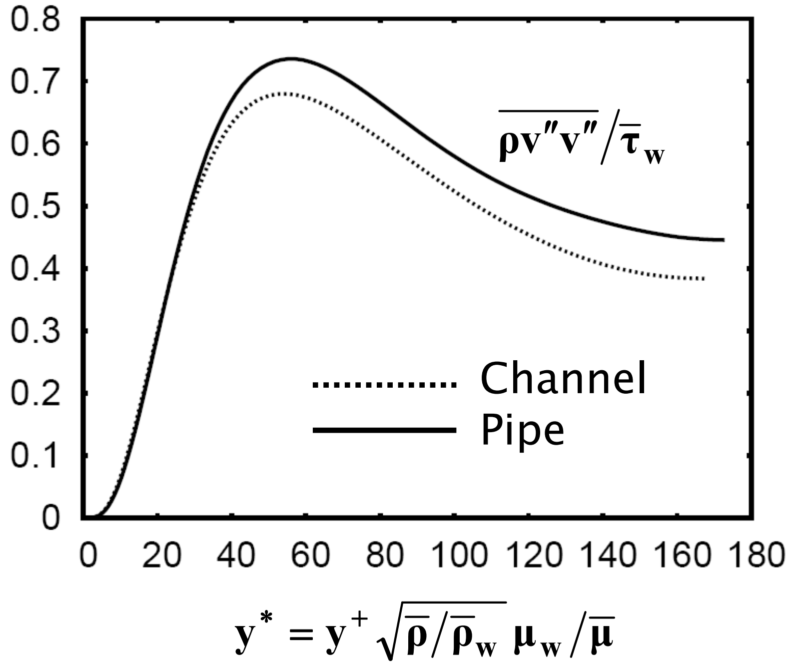

Similarity close to the wall. Wall-normal stress interacts with the mean pressure.

Streamwise Reynolds stress balance

Terms normalized with semi-local values $\tau_w^2/\mu(T)$

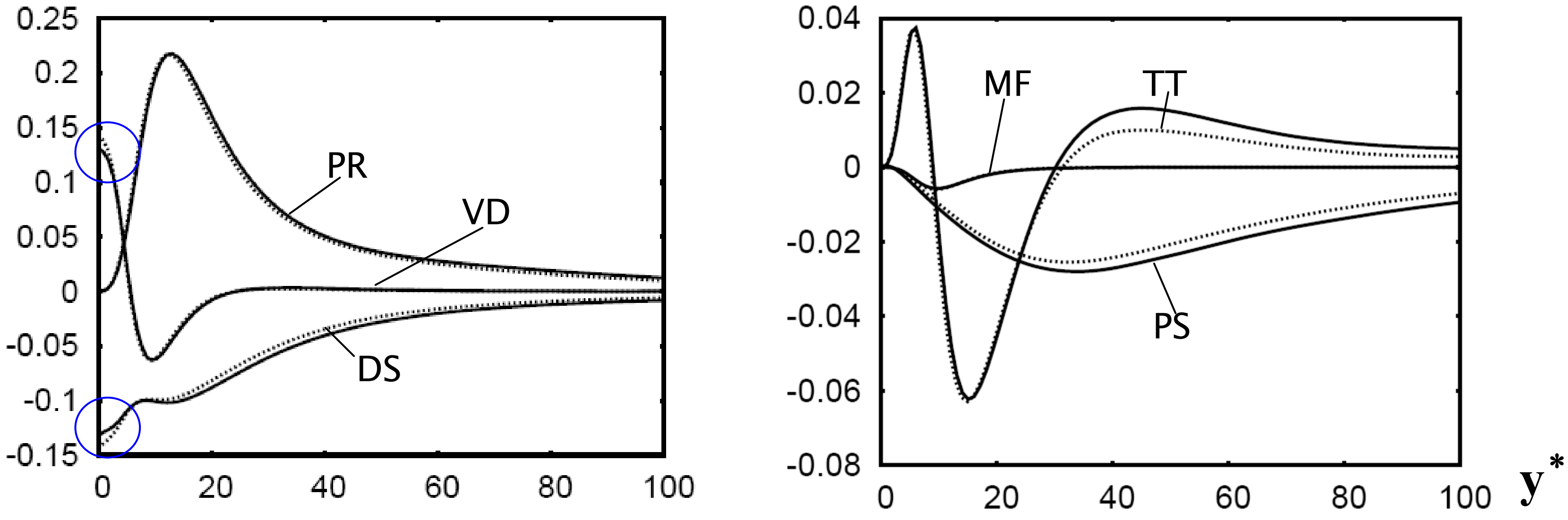

Similarity close to the wall, except for DS, VD (different curvature of u_{rms} in y-direction)

Reduced energy redistribution (PS) & TT in the channel core

RMS vorticity fluctuations

Terms normalized with τ_w/μ_w

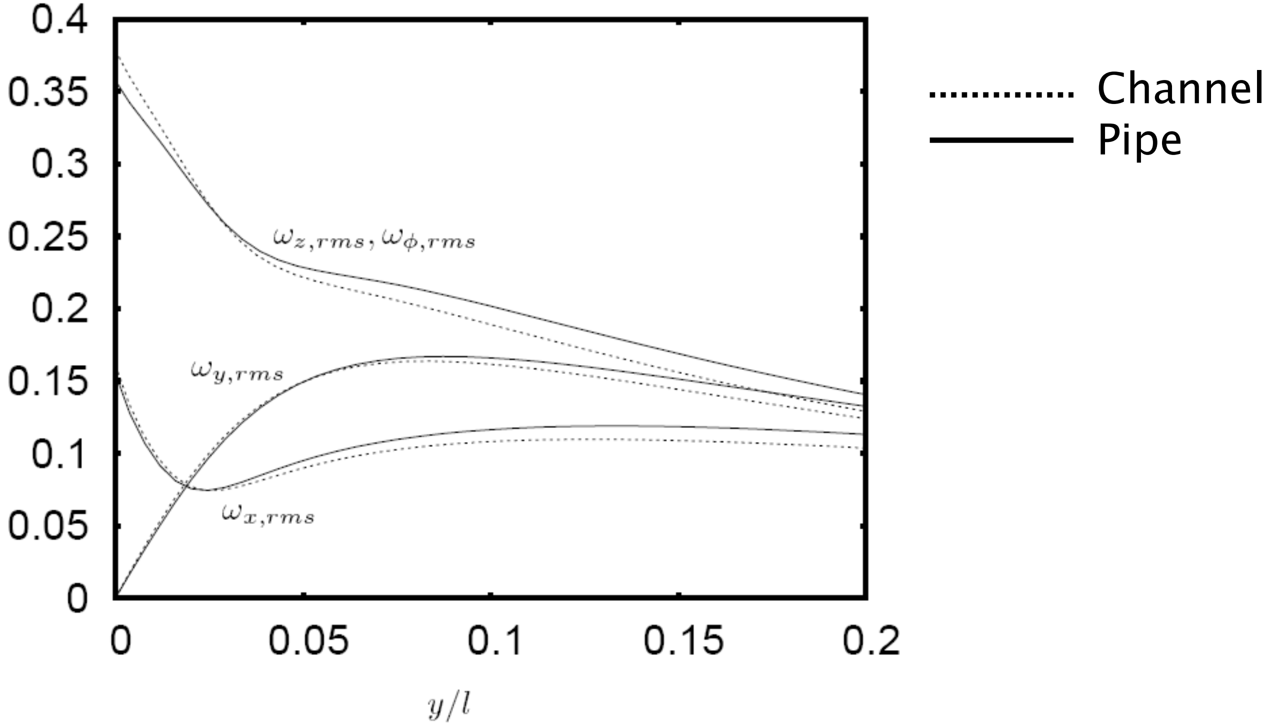

Different curvature of u_{rms} in y-direction close to the wall is also reflected in $\omega_z = \partial v'/\partial x - \partial u'/\partial y$

RMS pressure fluctuations

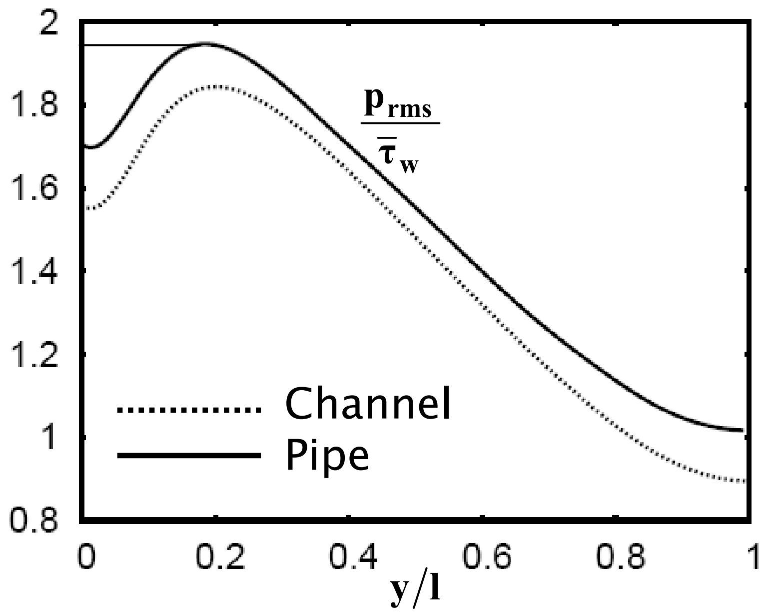

channel/pipe: compressible, Re_τ=245

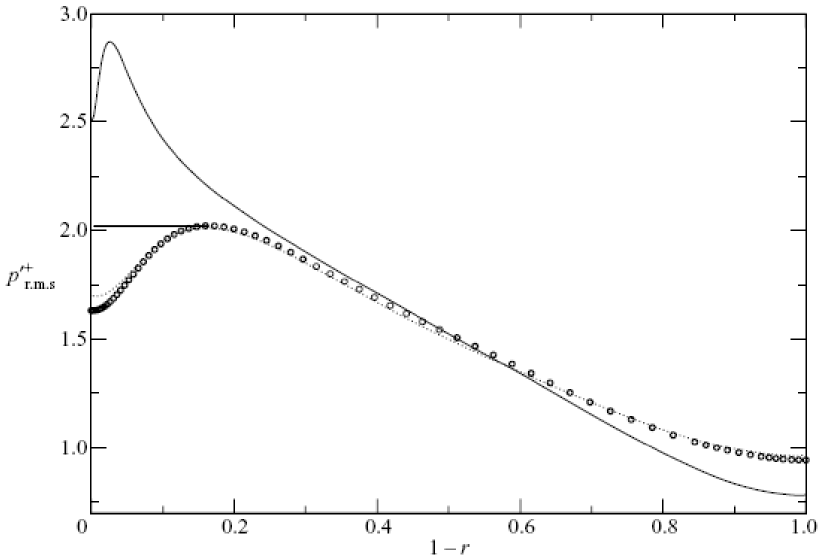

Wu & Moin (JFM 608, 2008)
Re_τ=180, 1142, incompressible pipe

Subtle differences between channel and pipe flow.
‚Compressibility‘ reduces pressure fluctuations in the wall layer.

Analysis of pressure fluctuations

Laplacian of pressure fluctuations in channel & pipe

$$\nabla^2 p' = \underbrace{-2\bar{\rho}\frac{\partial \tilde{u}_1}{\partial x_2}\frac{\partial u_2''}{\partial x_1}}_{A_R} \underbrace{-\bar{\rho}\frac{\partial^2}{\partial x_i \partial x_j}\left(u_i''u_j'' - \overline{u_i''u_j''}\right)}_{A_S} \underbrace{-2\frac{\partial \bar{\rho}}{\partial x_2}\frac{\partial}{\partial x_j}\left(u_2''u_j'' - \overline{u_2''u_j''}\right)}_{B_1} \underbrace{-\frac{\partial^2 \bar{\rho}}{\partial x_2^2}\left(u_2''^2 - \overline{u_2''^2}\right)}_{B_2}$$

$$\underbrace{-2\frac{\partial \tilde{u}_1}{\partial x_2}\frac{\partial}{\partial x_1}\left(\rho' u_2''\right)}_{C_1} \underbrace{-\frac{\partial^2}{\partial x_i \partial x_j}\left(\rho' u_i''u_j'' - \overline{\rho' u_i''u_j''}\right)}_{C_2} \underbrace{-\frac{D^2\rho'}{Dt^2}}_{C_3} + \underbrace{\frac{\partial^2 \tau_{ij}'}{\partial x_i \partial x_j}}_{V} \cong \bar{\rho} f'\,.$$

$$\nabla^2 p' = \underbrace{-2\bar{\rho}\frac{\partial \tilde{u}_x}{\partial r}\frac{\partial u_r''}{\partial x}}_{A_R} \underbrace{-\bar{\rho}\left(\frac{1}{r}\frac{\partial^2 r\left(u_r''u_r'' - \overline{u_r''u_r''}\right)}{\partial r^2} + \frac{2}{r^2}\frac{\partial^2 r u_r''u_\varphi''}{\partial r \partial \varphi} + \frac{1}{r^2}\frac{\partial^2 u_\varphi''u_\varphi''}{\partial \varphi^2} - \frac{1}{r}\frac{\partial\left(u_\varphi''u_\varphi'' - \overline{u_\varphi''u_\varphi''}\right)}{\partial r}\right)}_{A_S}$$

$$\underbrace{-\bar{\rho}\left(\frac{2}{r}\frac{\partial^2 r u_r''u_x''}{\partial r \partial x} + \frac{2}{r}\frac{\partial^2 u_\varphi''u_x''}{\partial \varphi \partial x} + \frac{\partial^2 u_x''u_x''}{\partial x^2}\right)}_{A_S} + B_1 + B_2 + C_1 + C_2 \underbrace{-\frac{D^2\rho'}{Dt^2}}_{C_3} + \underbrace{\nabla\cdot\nabla\cdot\underline{\underline{\tau}}'}_{V} \cong \bar{\rho} f'\,.$$

C_1–C_3 terms are small in supersonic channel and pipe flow

Analysis of pressure fluctuations

Variable density ansatz neglecting wave-propagation effects
(Poisson equation for pressure fluctuations in the pipe)

FT in homogeneous directions (x, ϕ):

$$\frac{d^2\hat{p}}{dr^2}+\frac{1}{r}\frac{d\hat{p}}{dr}-\left[k_x^2+\frac{1}{r^2}k_\varphi^2\right]\hat{p}=\overline{\rho}\,\hat{f}\quad \text{with b.c.}\quad \left.\frac{d\hat{p}}{dr}\right|_{r=1}=\frac{4}{3}\left(\overline{\mu}\frac{d^2\hat{u}_r}{dr^2}+\frac{d\overline{\mu}}{dr}\frac{d\hat{u}_r}{dr}\right)_{r=1}.$$

Replace r.h.s by $\delta(r-r_0)$ and compute the Green function G to obtain the solution of the Poisson equation

$$\hat{p}\left(k_x,r,k_\varphi\right)=\int_0^1\overline{\rho}(r_0)\,\hat{G}\left(k_x,k_\varphi,r,r_0\right)\hat{f}\left(k_x,k_\varphi,r_0\right)r_0\,dr_0+\hat{B}\left(k_x,k_\varphi,r\right)$$

The Green function $\hat{G}$ and the boundary condition $\hat{B}$ depend on modified Bessel functions.

Green function for channel and pipe flow

The Green function Ĝ for a point source at y/l=0.42 and 2 sets of wave-numbers decays faster in the pipe:

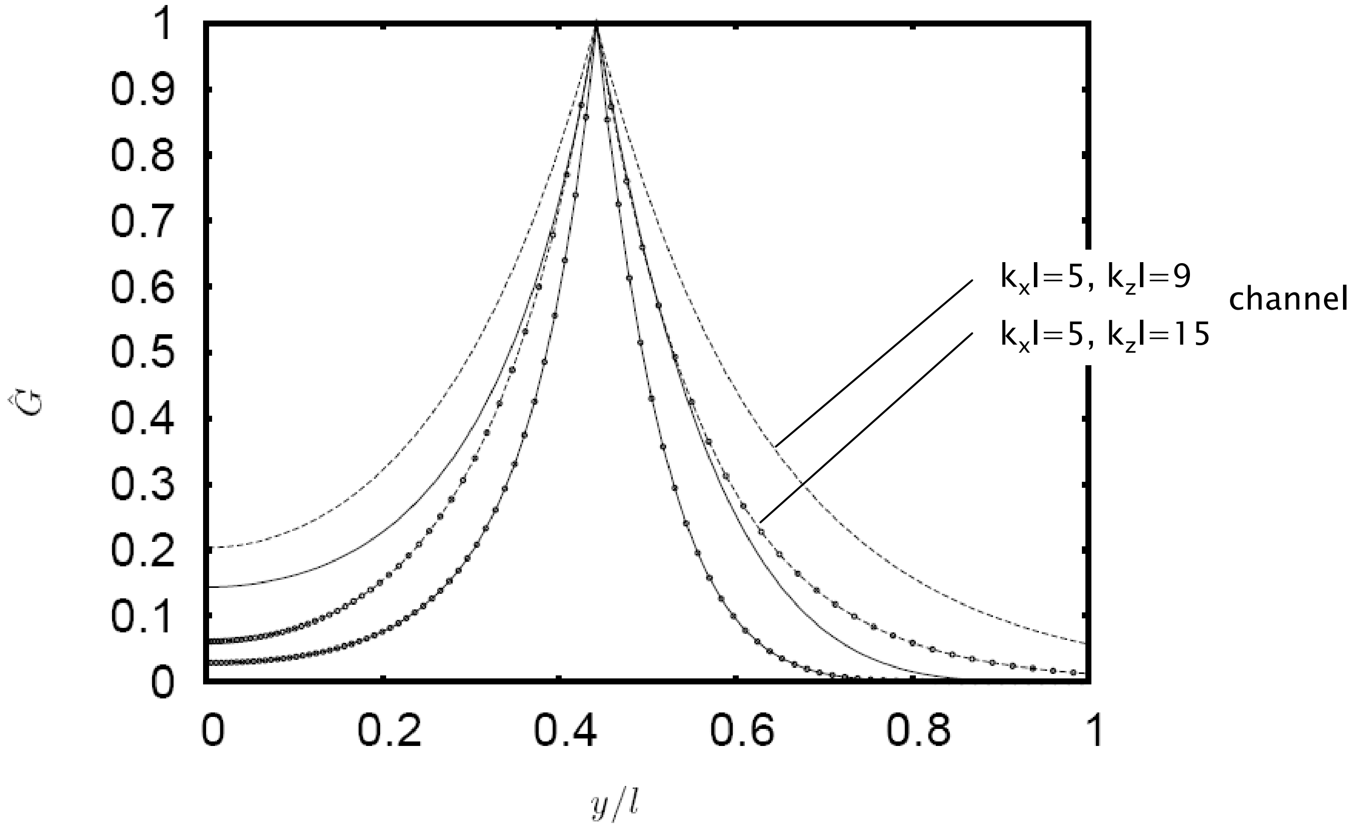

Green function solution for Π_{xx}

X-component of pressure-strain correlation for pipe flow:

$$\Pi_{xx}(r) = \overline{p'\frac{\partial u'}{\partial x}}(r) = \int_0^1 \overline{\rho}(r_0)\,\overline{G * f'(x, r, \varphi; r_0)\frac{\partial u'}{\partial x}}\, r_0 dr_0 \;+\; \overline{B'\frac{\partial u'}{\partial x}}$$

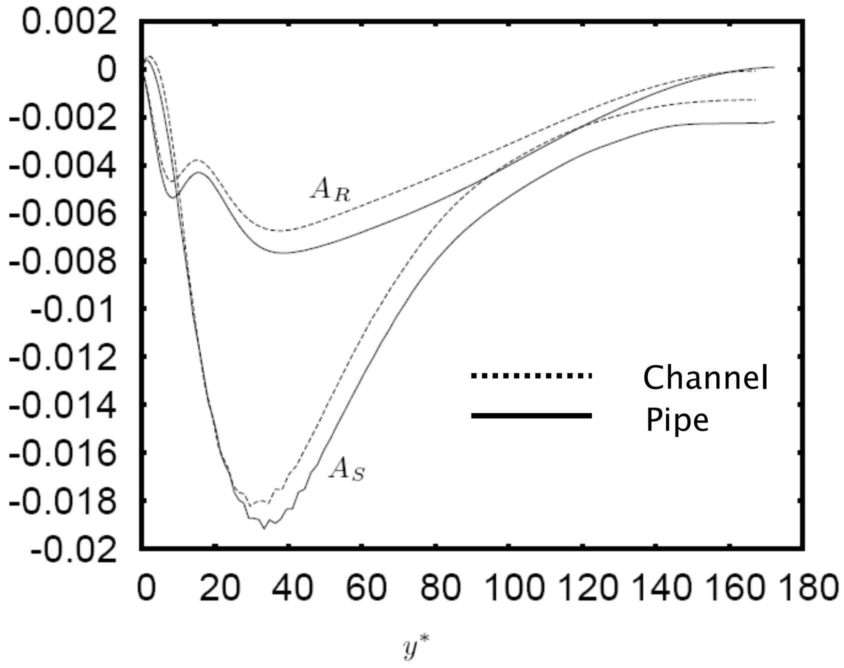

Contributions of rapid and slow terms

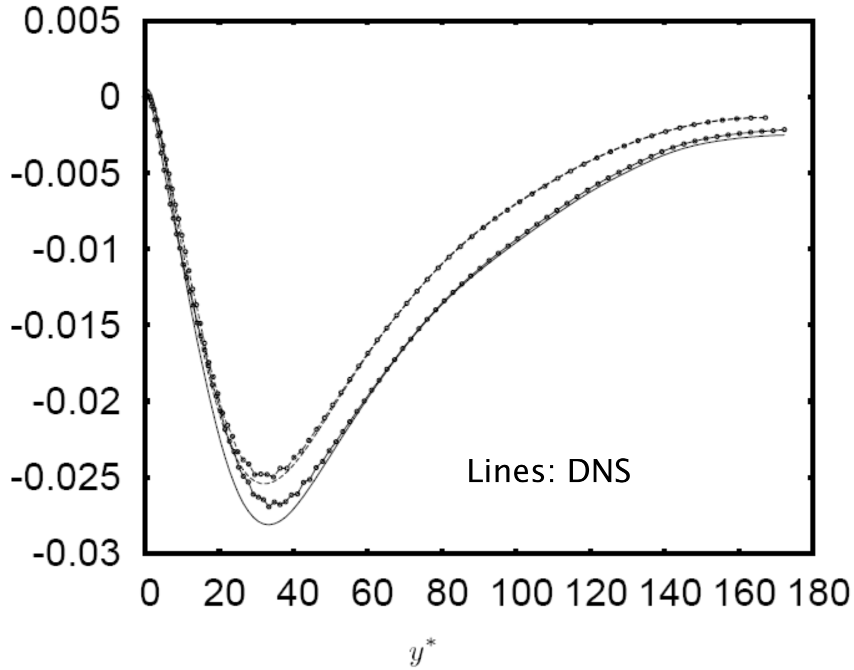

all terms

Differences are due to different mean densities!

Summarizing remarks

- Supersonic turbulent channel and pipe flows were compared at equal friction Reynolds and Mach numbers

- DNS data reveal more differences than similarities between both flows

- Differences in mean property variations are due to transverse curvature and loose importance as the Re-number increases

- Differences in mean density directly affect pressure-strain correlations. Challenge for turbulence modelling!